Chapter 4

Structure of Mesh Phases : Influence of the Hydrophilic Head Group of the Surfactant and the Nature of the Counterions

4.1 Introduction

The important role of the length of the hydrocarbon chain of the surfactant in stabilizing different liquid crystalline phases between the hexagonal and lamellar is well studied. Shorter hydrocarbon chains generally induce the bicontinuous cubic phase (V_1), whereas longer ones induce other intermediate phases (*Int*), such as ribbon and mesh phases [1]. The *Int* phases are also seen with surfactants with stiffer fluorocarbon chains. The headgroup size which determines the interfacial curvature is also an important factor in stabilizing the V_1 or *Int* phases [2]. Basically a balance between the aggregate flexibility, determined by the chain length, and the interfacial curvature seems to decide which of these structures is formed. Both of them can be tuned using either a co-surfactant or an adsorbing counterion in the case of ionic surfactants [3, 4].

In chapters 2 and 3, we have described the phase behaviour of the CTAB-SHN-water system. It is found to show a rich phase behaviour with a random two dimensional (2-D) mesh phase and a 3-D ordered mesh phase with rhombohedral symmetry at higher surfactant concentrations. DTAB, which is a shorter chain analogue of CTAB, forms only the 2-D random mesh phase, but not the 3-D ordered one. In this chapter we investigate the role of different head groups on the structure and stability of these phases, keeping the chain length same as that of CTAB. The surfactant used is cetylpyridinium bromide (CPB). In section 4.2, earlier studies on this kind of systems have been

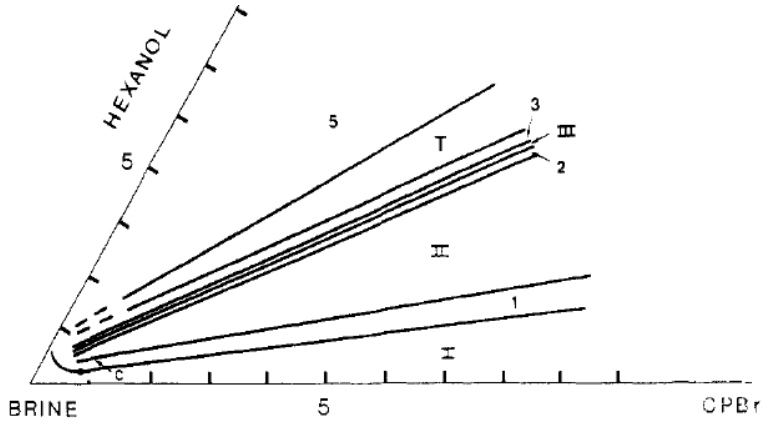

Figure 4.1: The phase diagram of CPB-hexanol-brine (0.2 M NaBr) system. The mesophasic domains are isotropic (I), lamellar liquid crystal (II) and isotropic sponge (III) [7].

presented. Like CTAB, CPB shows the 2-D hexagonal phase over a wide concentration range. The experimental techniques are briefly discussed in section 4.3, and our results are described in section 4.4. For low amounts of added 3-sodium-2-hydroxy naphthoate (SHN), the phase diagram is very similar to that of the CPB-water binary system. Higher salt content induces a lamellar phase with curvature defects. Interestingly, the mesh-like aggregates forming this phase have a four-fold symmetry axis normal to the plane, instead of the hexagonal symmetry seen in the mesh phases of the CTAB-SHN system. At still higher surfactant concentrations, an ordered mesh phase is formed, where the square mesh-like aggregates order in three dimensions in a body centred lattice. The three component phase diagram is found to be symmetric about the equimolar CPB-SHN composition.

To check the effect of the surfactant counterion, the phase diagram of the cetylpyridinium chloride (CPC)-SHN-water system has been determined. At equimolar composition this system forms a regular lamellar phase. No mesh phases are found in this system, indicating the importance of specific ion effects in stabilizing these phases.

Further the effects of the strongly bound counterion was probed by adding sodium salicylate (SS) and sodium *p*-toluene sulfonate (ST) to CPB. Both these salts give a very different phase diagram from that of SHN, as described in section 4.5. These two salts do not alter the cylindrical morphology of the surfactant aggregates found in the CPB-water binary system. The conclusions that may be drawn from these studies are given in the last section.

4.2 Earlier studies

Like most surfactant systems, CPB and CPC form spherical micelles just above the CMC. Further increase in the surfactant concentration gives rise to cylindrical micelles. In the concentrated region the phase diagram is dominated by the 2D hexagonal phase.

In the dilute regime, CPB micelles are found to grow in to large flexible cylinders with increasing NaBr while CPC micelles remain small and globular with NaCl [5, 6]. The influence of hexanol on the phase behaviour of CPB and CPC in brine has been investigated [7]. With increasing hexanol content, the following phase sequence is observed: isotropic micellar solution (L_1) $\rightarrow$ lamellar liquid crystalline phase (LLC) $\rightarrow$ sponge phase (Fig. 4.1). The sponge phase is an optically isotropic phase which scatters light and exhibits streaming birefringence . This sequence is same for both the surfactants and found to be quite general [8]. In the organic solvent, *N*-methylsydnone, CPB is found to form hexagonal and lamellar phases [9]. All of the above studies are confined to the dilute regime.

The intermediate phases which provide a fascinating topological link between hexagonal and lamellar phases is an interesting subject in the field of lyotropic liquid crystals. There are many systems which show the presence of such phases [10], where lamellae containing water filled holes (mesh structure) may or may not be correlated from one layer to the next [11, 12, 13]. In some systems the development of out of plane positional correlations of the mesh-like aggregates at high surfactant concentrations leads to the formation of the intermediate mesh phase with 3-D tetragonal or rhombohedral lattice [14]. A more detailed description of earlier work on mesh phases has been given in the previous chapter (section 3.2).

4.3 Experimental

The surfactants CPB and CPC and organic salts SS and ST were purchased from Aldrich. SHN was prepared as described in chapter 2. The chemical structures of the molecules are given in figure 4.2. The experimental techniques used to identify the different phases were same as those described in previous chapters.

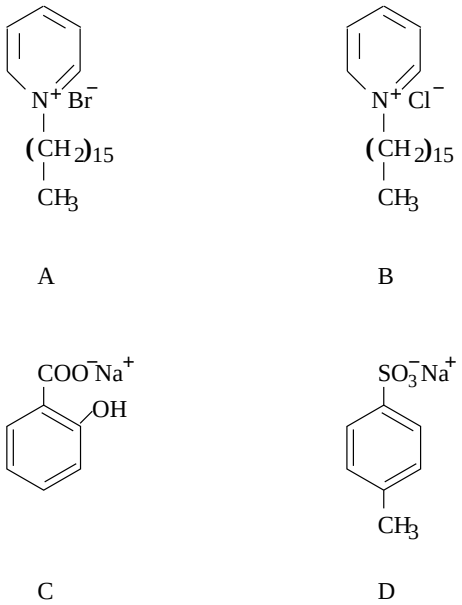

Figure 4.2: Chemical structure of (A) cetylpyridinium bromide, (B) cetylpyridinium chloride, (C) sodium salicylate and (D) sodium tosylate.

The phase behaviour of the systems were probed as a function of the molar ration α of the organic salt to the surfactant, and of the total concentration of the surfactant and salt (ϕ_s). The temperature was varied from 30 to 80 ° C.

4.4 Results

4.4.1 CPB-SHN-water system

For this system α was varied from 0.25 to 2.0 and for each α, ϕ_s was varied from 10 to 80 wt%. To draw the three component phase diagram, around 100 compositions were characterized.

4.4.1.1 Phase behaviour at α = 0.25

At this small amount of added salt, the phase behaviour is very similar to that of the binary CPB-water system. The viscoelastic isotropic phase (I) which shows slight flow birefringence is made up of cylindrical micelles. At higher ϕ_s, this isotropic phase transforms to an aniosotropic liquid crystalline phase through a two phase region (Fig. 4.3). The typical texture of this phase under crossed polarizers is shown in figure 4.4. X-ray diffraction shows two peaks with the magnitude of scattering vector q in the ratio $1 : \sqrt{3}$. These reflections correspond to the (10) and (11) planes of

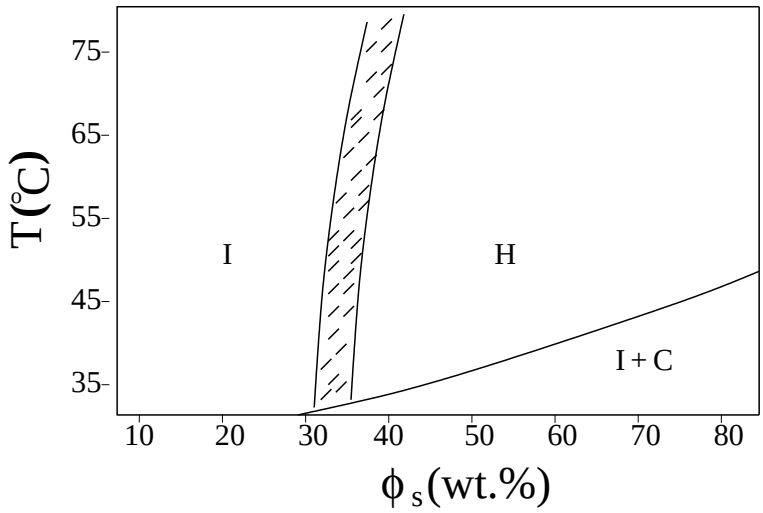

Figure 4.3: Phase diagram of CPB-SHN-water system at $\alpha = 0.25$. I, H and C denote the isotropic, hexagonal and crystalline phases, respectively. The shaded regions in all the phase diagrams correspond to two-phase regions.

a 2-D hexagonal lattice. The Kraft temperature is found to increase with ϕ_s.

4.4.1.2 Phase behaviour at α = 0.5 and 1.0

Over a wide range of concentration ($\phi_s \leq 35$) a lamellar phase coexists with an isotropic phase for $\alpha = 0.5$ (Fig. 4.5). The isotropic solution is found to float on top of the lamellar phase. The typical oily streak texture shown by this sample is characteristic of lamellar phase (Fig. 4.6). X-ray diffraction pattern of this phase shows three peaks with their q values in the ratio $1 : 2 : 3$. These reflections are observed along q_z where z is the direction of lamellar stacking. In the perpendicular direction, along $q_\perp$ there is a diffuse peak at a lower q value (similar to Fig. 4.11A). This diffuse reflection is attributed to curvature defects in the plane of the bilayer. On increasing the temperature at these concentrations the lamellar phase (L_α^D) disappears leaving only the single isotropic phase. The transition temperature increases with ϕ_s.

On further increase of ϕ_s a mosaic microscopy texture is observed, which is different from that of other lyotropic liquid crystalline phases (Fig. 4.7). On heating this texture transforms into the characteristic texture of lamellar phase with a narrow temperature range over which both of them coexist. It is also found that the homeotropically aligned regions in lamellar texture (which appear dark under crossed polarizers) persist even on cooling the sample to the phase with the

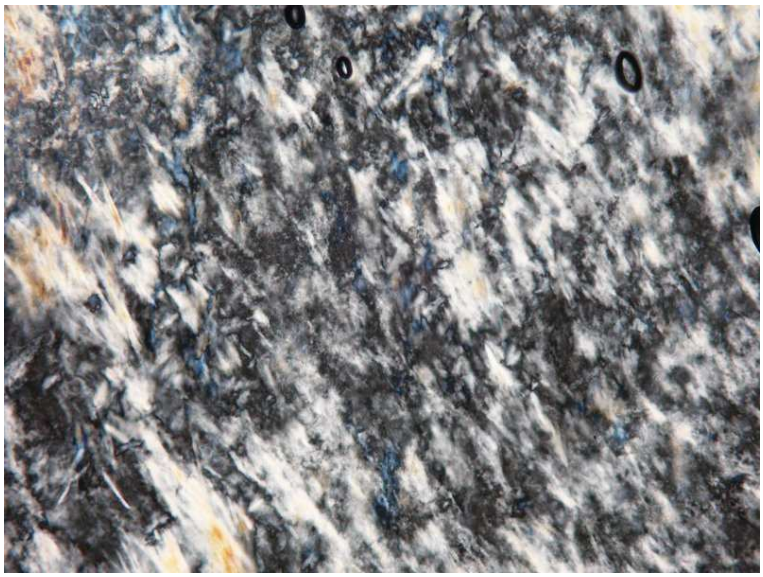

Figure 4.4: Typical texture of hexagonal phase of CPB-SHN-water system under crossed polarizers at α = 0.25, ϕ_s = 60 and T = 45° C.

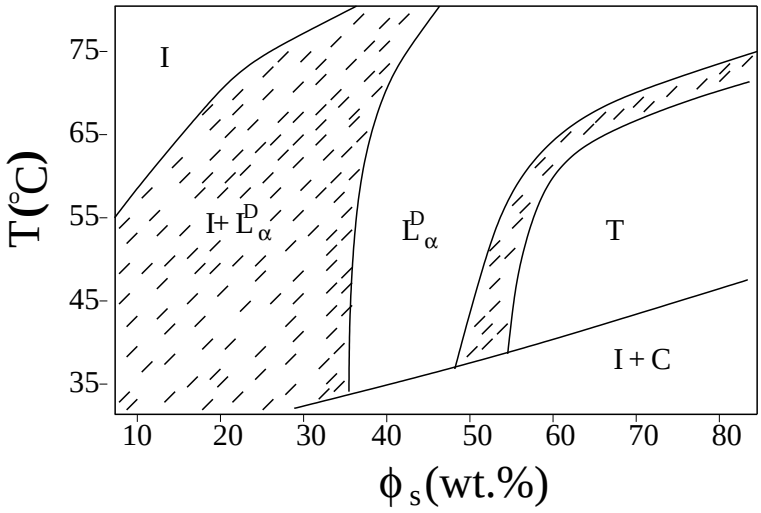

Figure 4.5: Phase diagram of CPB-SHN-water system at α = 0.5. I, L^D_α, T and C denote the isotropic, lamellar with curvature defects, tetragonal and crystalline phases, respectively.

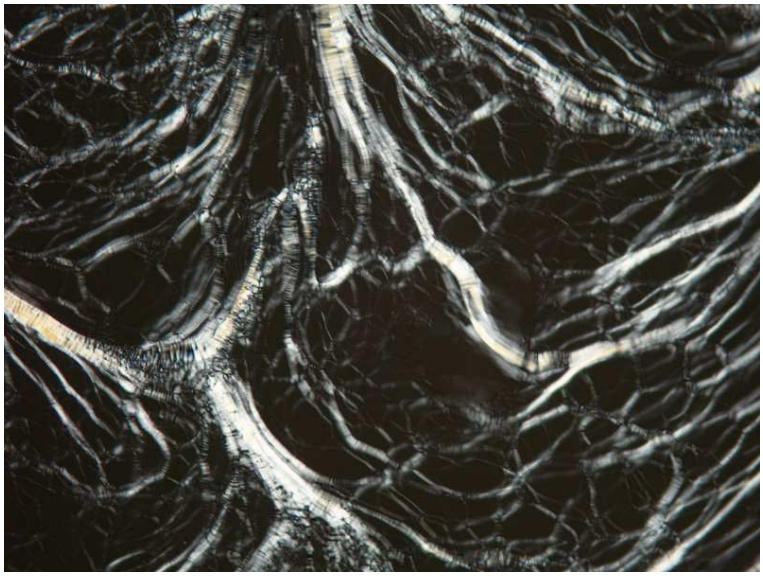

Figure 4.6: Typical texture of lamellar phase (L_α^D) of CPB-SHN-water system under crossed polarizers at α = 0.5, ϕ_s = 20 and T = 30° C.

mosaic texture. The transition temperature increases with increasing ϕ_s. X-ray diffraction pattern of this phase show six peaks suggesting a more ordered structure than the lamellar phase. Careful observations reveal that the diffuse peak in the L_α^D phase becomes more intense and it splits into four spots as ϕ_s is increased (Fig. 4.8). These reflections could be indexed on to a body centred tetragonal lattice (Table 4.1). On heating the diffraction pattern of this phase (T) changes and shows two peaks corresponding to a lamellar periodicity along with the four diffuse spots (similar to Fig. 4.11B). On further heating the four spots merge into a diffuse ring (similar to Fig. 4.11A). The T phase is found upto the highest composition investigated ($\phi_s \sim 80$), and a regular lamellar phase is never observed.

The sequence of phases appearing in the phase diagram at α = 1.0 is the same as that at α = 0.5 (Fig. 4.9). The Kraft temperature seems to come down with the higher amount of added SHN. Another remarkable feature is the shift of the L_α^D - T phase boundary towards higher values of ϕ_s, giving rise to the presence of the L_α^D phase over a wider range of surfactant concentrations.

4.4.2 Phase behaviour at α = 1.35

For this composition, the isotropic phase exists over a wider range of surfactant concentration (Fig. 4.10). A lamellar phase coexists with the isotropic phase over a narrow range of ϕ_s. At

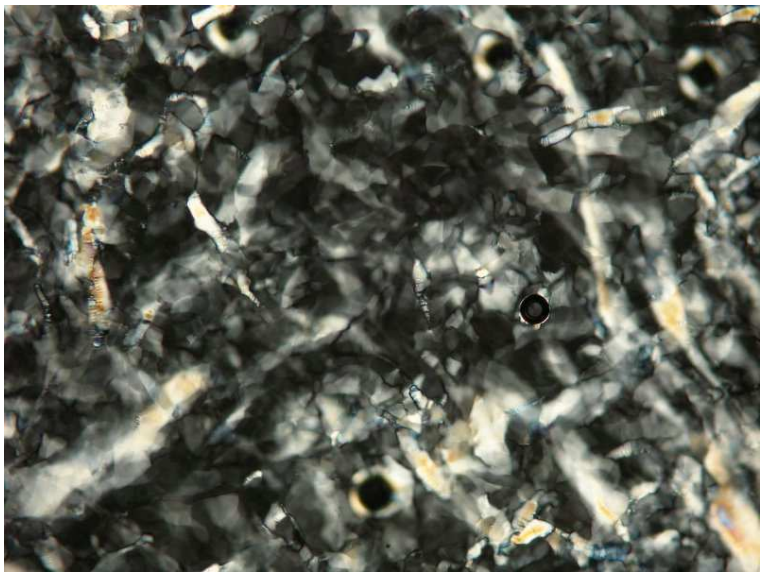

Figure 4.7: Typical texture of tetragonal (T) phase of CPB-SHN-water system under crossed polarizers at α = 0.5, ϕ_s = 70 and T = 50° C.

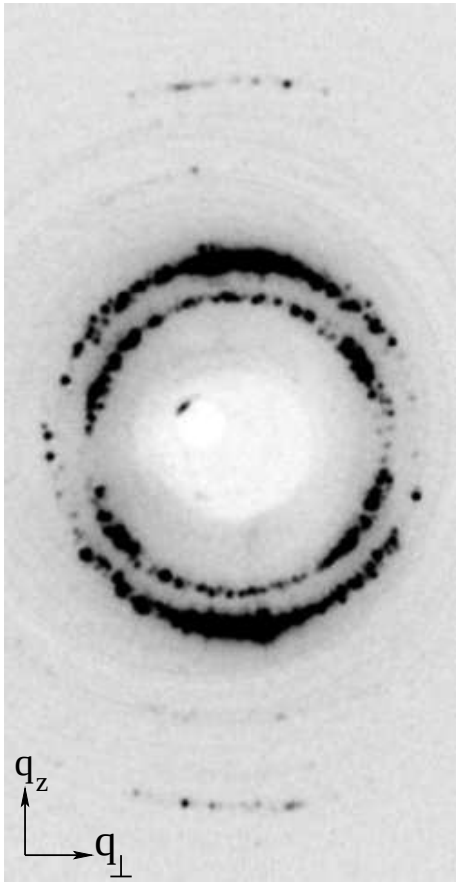

Figure 4.8: Diffraction pattern of a partially aligned sample in the tetragonal phase at α = 0.5, ϕ_s = 80 and T = 45° C.

Table 4.1: X-ray diffraction data from the tetragonal phase of the CPB-SHN-water system at α = 0.5 and ϕ_s = 80, indexed on a 3-D body centred tetragonal lattice. The calculated spacings (d_{calc}) are obtained from the relation, $(1/d)^2 = (h^2 + k^2)/a^2 + l^2/c^2$ with the condition $h+k+l = 2n$, where n is an integer. The unit cell parameters are a = 6.70 nm and c = 8.43 nm.

d_{exp}(nm)	d_{calc}(nm)	plane	intensity
5.25	5.25	(101)	vs
4.22	4.22	(002)	vvs
2.81	2.82	(211)	w
2.37	2.37	(220)	w
2.13	2.11	(04)	s
1.43	1.41	(006)	w

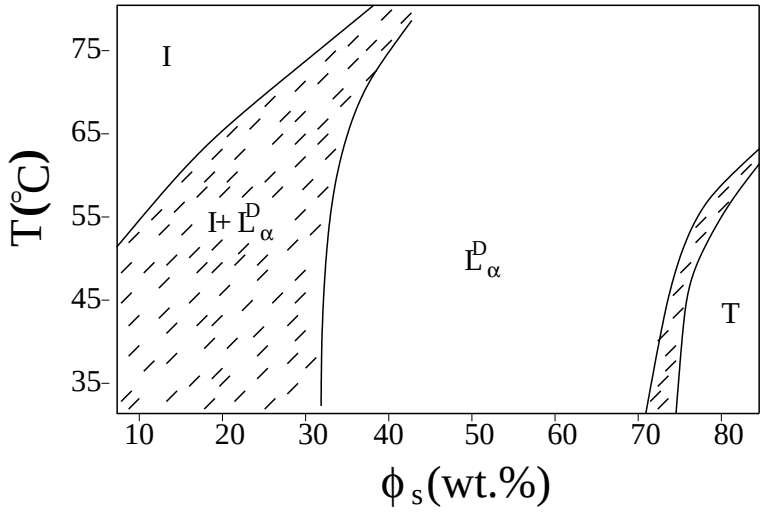

Figure 4.9: Phase diagram of CPB-SHN-water system at α = 1.0. The symbols are same as in figure 4.5.

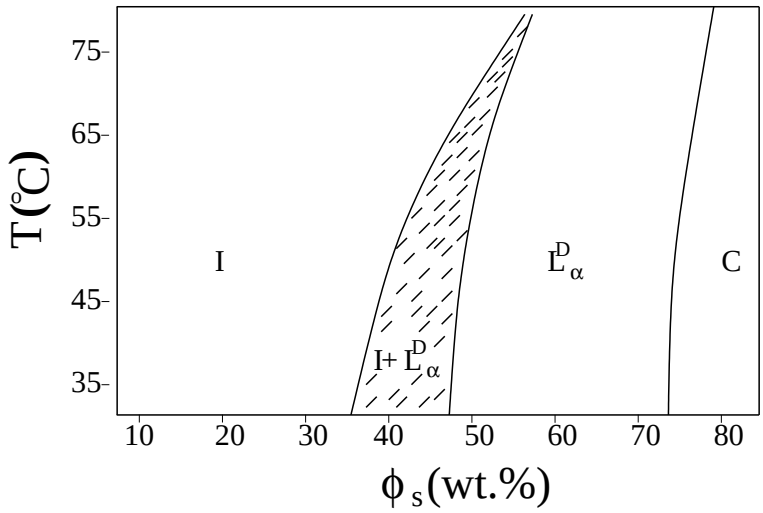

Figure 4.10: Phase diagram of CPB-SHN-water system at α = 1.35. The symbols are same as in figure 4.5.

Table 4.2: Variation of lamellar periodicity (d) and average defect separation (d_d) in CPB-SHN-water system at α =1.35 and T = 30°C.

ϕ_s	$d(nm)$	$d_d(nm)$
40	6.62	-
50	5.81	6.42
60	5.12	6.12
70	4.53	5.45

higher ϕ_s, a single lamellar phase is observed, whose diffraction pattern shows a diffuse peak in the $q_\perp$ direction, along with the lamellar peaks along q_z. With further increase of ϕ_s, the diffuse peak again splits into four intense spots (Fig. 4.11A & B). Even at higher ϕ_s this L_α^D phase does not transform into an ordered T phase. The lamellar periodicity and the corresponding defect position for different ϕ_s are shown in table 4.2. Both these parameters are found to decrease with increasing ϕ_s.

4.4.2.1 Phase behaviour at α = 2.0

The phase behaviour at these high values of α is very similar to that at very low α (~ 0.25) (Fig. 4.12). At lower ϕ_s there is an isotropic viscoelastic gel which transforms to a 2D hexagonal phase on increasing ϕ_s. At much higher ϕ_s the added SHN does not mix with the sample and crystallizes

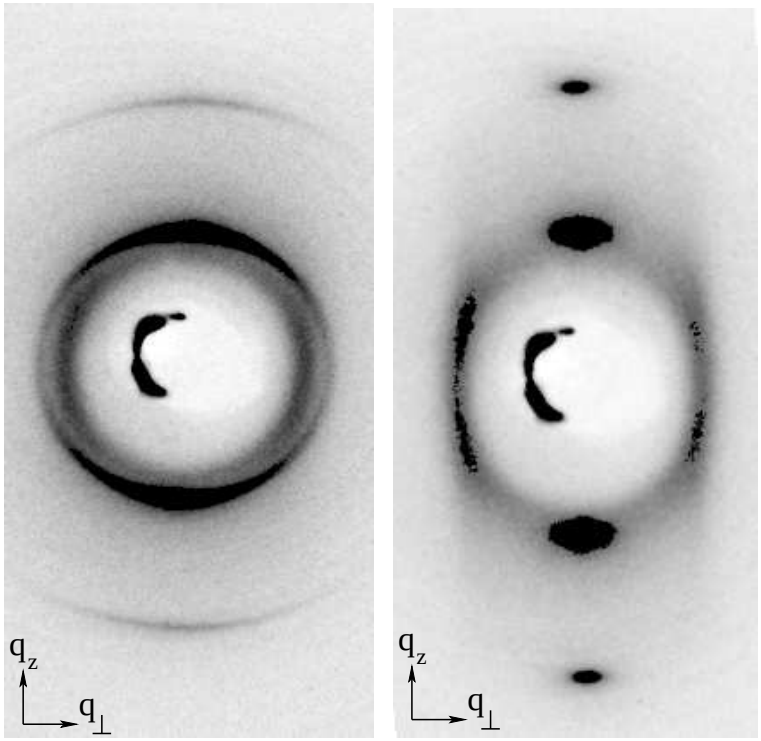

A B

Figure 4.11: Diffraction pattern of L_α^D phase in CPB-SHN-water system at α = 1.35, T = 30° C and ϕ_s = 60 (A) and 70 (B), respectively.

out.

The overall ternary phase diagram is shown in figure 4.13. It is to be noted that the diagram is quite symmetric about the equimolar axis of CPB and SHN. Such a behaviour is quite common in oppositely charged mixed surfactant systems [3]. Although SHN is not a surfactant, the effect seems to be analogous to that of a surfactant.

4.4.3 CPC-SHN-water system

For this system the different phases were characterized at equimolar ratio of CPC and SHN (α = 1). ϕ_s was varied from 10 to 80 wt%.

Over a wide range of ϕ_s the lamellar phase is found to coexist with an isotropic solution (Fig. 4.14). The microscopy texture of this phase is similar to that of the lamellar phases in other systems. But the x-ray diffraction pattern of this phase is different in one respect (Fig. 4.15). It contains only a set of lamellar peaks with their scattering vectors in the ratio 1: 2: 3 along q_z;

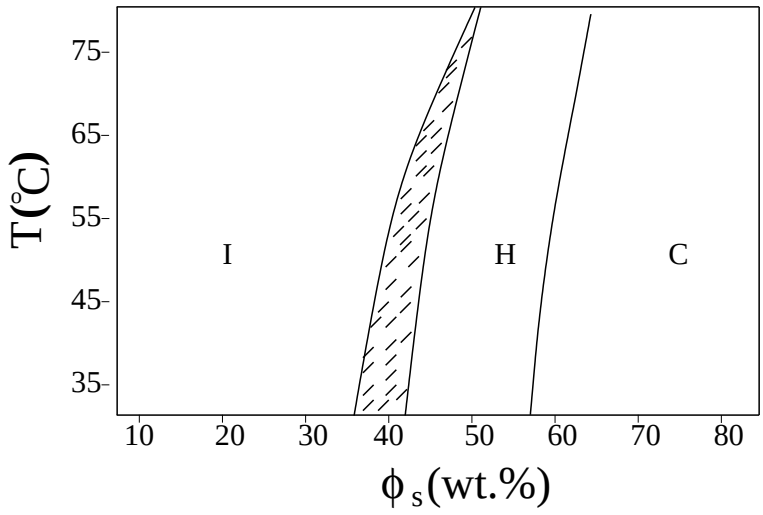

Figure 4.12: Phase diagram of CPB-SHN-water system at α = 2.0. The symbols are same as in figure 4.3.

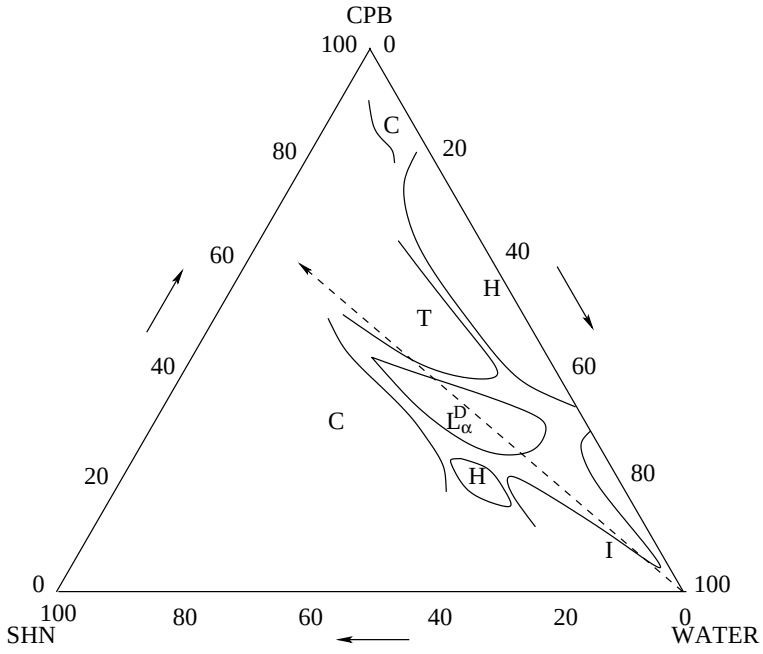

Figure 4.13: Partial ternary phase diagram of CPB-SHN-water system at 30° C. The concentrations are in wt%. I, H, L_α^D, T and C are the isotropic, hexagonal, lamellar with curvature defects, tetragonal and crystalline phases, respectively. The dashed line indicates the line of equimolar composition of CPB and SHN.

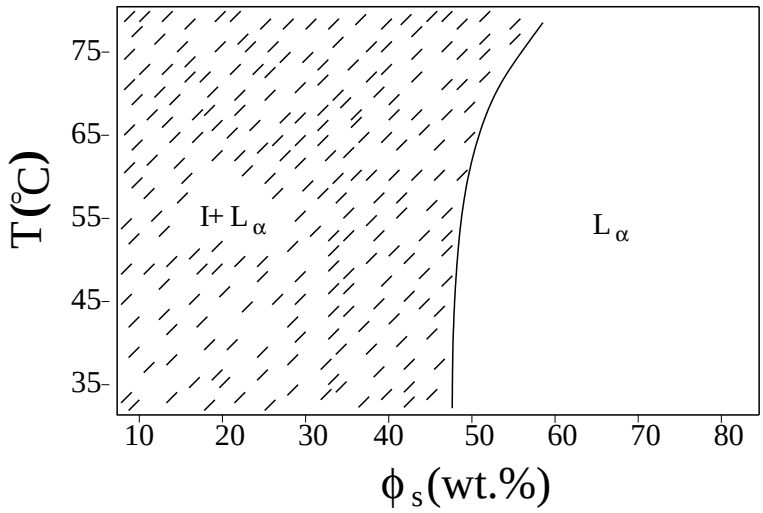

Figure 4.14: Phase diagram of CPC-SHN-water system at α = 1.0.

Table 4.3: Phases and variation of lamellar periodicity with ϕ_s in CPC-SHN-water system at T = 30° C.

ϕ_s	phase	$d(nm)$
10	$I + L_\alpha$	4.65
20	$I + L_\alpha$	4.79
30	$I + L_\alpha$	4.95
40	$I + L_\alpha$	5.38
50	L_α	5.30
60	L_α	5.52
70	L_α	4.94
80	L_α	4.30

there are no diffuse peaks in the normal direction. For $\phi_s \leq 60$, the bilayer separation is observed to increase with the addition of more surfactants by around 8 Å whereas for $\phi_s \geq 65$ it starts to decrease (Table 4.3). With temperature this phase also swells by a few Å for $\phi_s \leq 50$.

4.4.4 CPB-SS/ST-water system

For the CPB-SS system the phase diagram at α = 1.0 is shown in figure 4.16. At low ϕ_s, there is an isotropic gel. The phase diagram is dominated by the presence of the 2-D hexagonal phase. For this phase the x-ray diffraction pattern shows three reflections with their q in the ratio $1 : \sqrt{3} : 2$

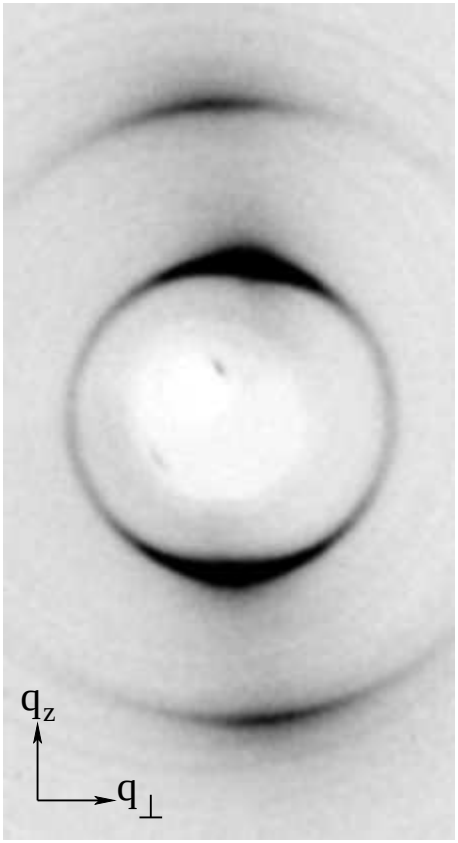

Figure 4.15: Diffraction pattern of L_α phase in CPC-SHN-water system at α = 1.0, ϕ_s = 60 and T = 30° C.

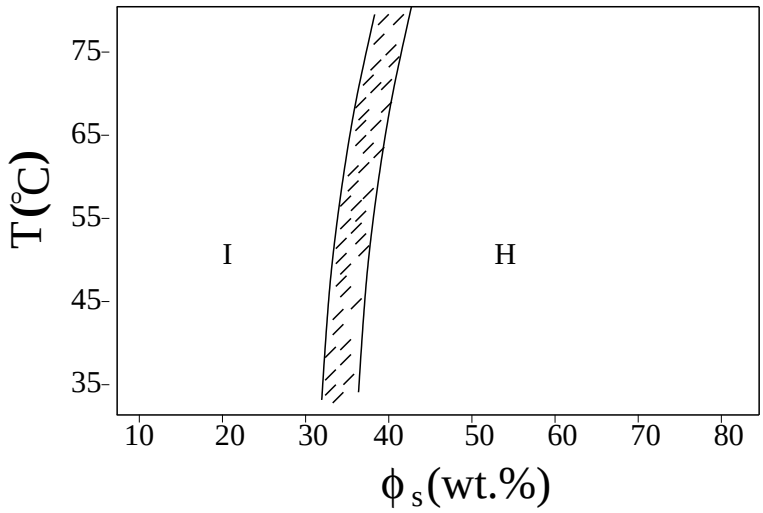

Figure 4.16: Phase diagram of CPB-SS-water system at α = 1.0.

(Fig. 4.17). No other liquid crystalline phases is observed in CPB-SS system. The phase diagram is quite similar to that of CPB-water binary system.

The phase diagram of CPB-ST is very similar to that of the CPB-SS system, and the lattice parameter of the hexagonal phase is also found to be similar (Table 4.4). With the addition of more and more surfactant the cylindrical micelles come closer and the lattice parameter reduces.

4.5 Discussion

4.5.1 Hexagonal and regular lamellar phases

Low amounts of SHN in CPB induce an isotropic viscoelastic gel. Observation of flow birefringence suggests the formation of worm-like micelles. Such behaviour is quite common in ionic surfactants when simple inorganic as well as organic salts are added to increase the length of cylindrical micelles [15, 16, 17, 18]. Further increase in ϕ_s brings the cylindrical micelles closer to arrange on a two dimensional hexagonal lattice. The hexagonal phase in the CPC-water system becomes unstable with the addition of SHN and transforms into a regular lamellar phase. Similar observations have been made in many other surfactant systems [4, 19]. The instability of the hexagonal phase is due to the screening of electrostatic interactions of the head groups, leading to a decrease in the curvature of the surfactant-water interface. The absence of any curvature defects in the plane of the bilayer in CPC-SHN system can be attributed to the high affinity of Cl^- ions

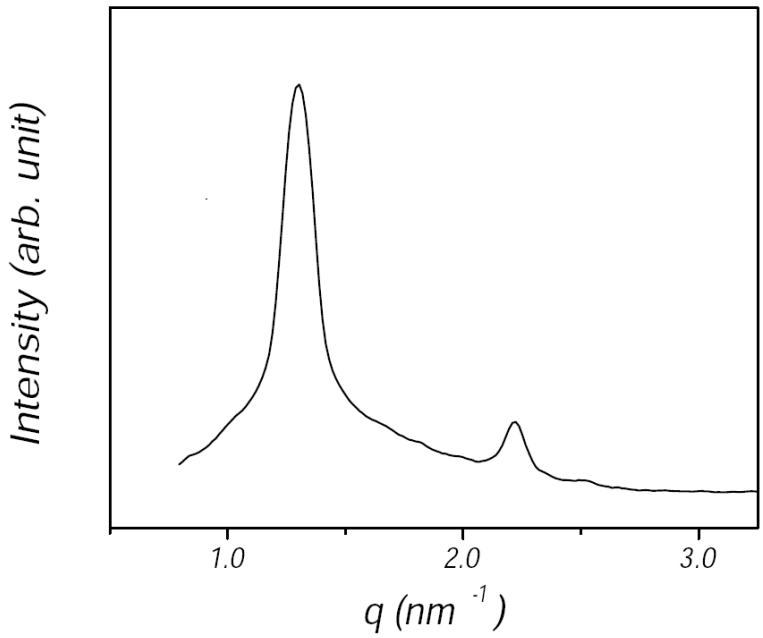

Figure 4.17: Typical diffraction pattern of hexagonal phase of CPB-SS-water system at α = 1.0, ϕ_s = 60 and T = 30° C.

to dissociate into water. It, therefore, becomes difficult to maintain the two different types of local environments necessary to form curvature defects. On the other hand, Br^- ions only partially dissociate from the surfactant aggregates, and hence these systems are better thought of as made up of two species. Hence it becomes possible to maintain the two different micro-environments necessary to stabilize curvature defects in CPB-SHN system. Such ion specific behaviour has been discussed in more detail in previous chapters and in [20]. The increase of lamellar periodicity with increasing ϕ_s within the isotropic-lamellar coexistence region of the CPC-SHN system may be due to a decrease in the osmotic pressure applied by the isotropic phase. A similar observation has been discussed in chapter 2. The reappearance of the hexagonal phase at much higher α in the CPB-SHN system produces a symmetric three component phase diagram. The analogous phase behaviour at low and high α can be explained by the presence of highly charged aggregates, although of opposite signs.

4.5.2 Structure of the mesh phases

The diffraction pattern of the lamellar phase found at lower ϕ_s contains a diffuse peak along $q_\perp$, which cannot be produced by a regular bilayer. It implies the presence of structural defects in the

Table 4.4: Different mesophases in CPB-ST-water system at α = 1.0.

ϕ_s	d_1	d_2	d_3	phase	lattice parameter
36	very diffuse	-	-	I	-
49	5.19	3.01	-	H	5.99
60	4.63	2.71	2.35	H	5.34
80	4.29	2.48	-	H	4.95

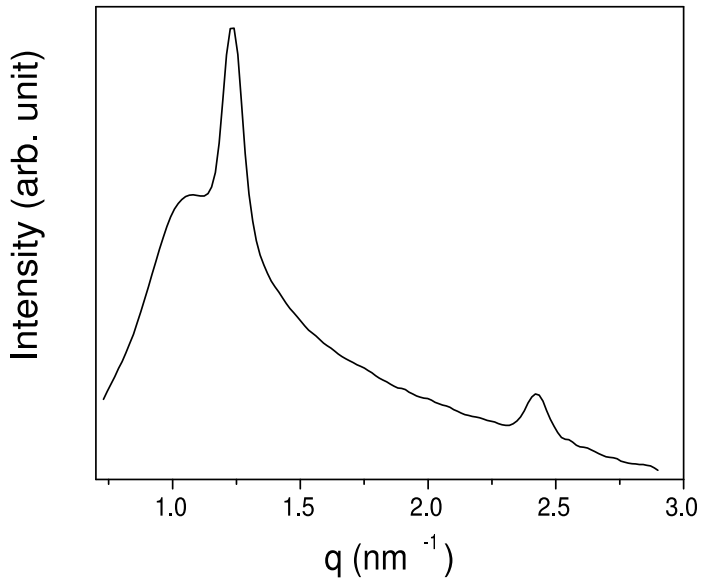

Figure 4.18: X-ray diffraction pattern of the lamellar phase with curvature defects in the CPB-SHN system at α = 1.35, ϕ_s = 60 and T = 30° C.

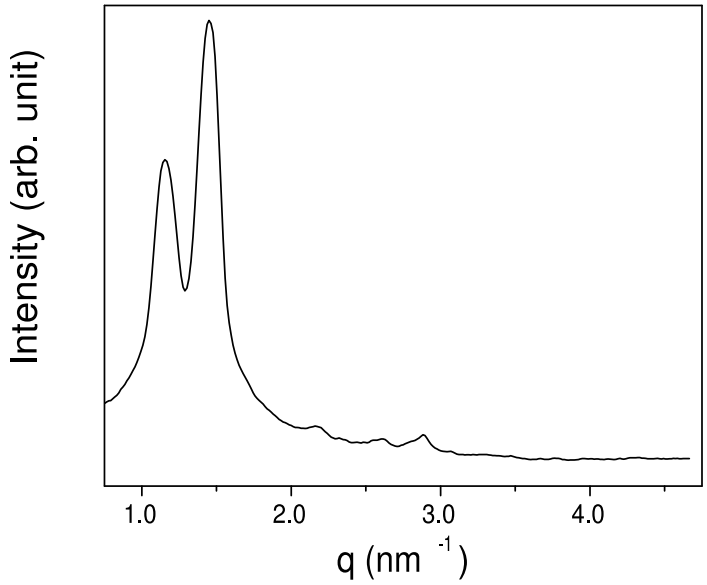

Figure 4.19: X-ray diffraction pattern from the tetragonal phase in CPB-SHN-water system at α = 0.5, ϕ_s = 70 and T = 40° C.

plane of the bilayer. On decreasing the water content, diffraction patterns from aligned samples show the diffuse peak becoming more sharp and then splitting into four spots (Fig. 4.11). It indicates the development of positional correlations of the defects across the bilayers (along q_z). As the bilayers are brought still closer, by decreasing the water content further, the defects get locked in to a 3-dimensional lattice, which is manifested by the presence of many reflections in the diffraction pattern. Figure 4.18 shows the peak coming from the structural defect in the plane of the bilayer, which is found to be much broader than the corresponding peak arising from the ordered structure at higher ϕ_s (Fig. 4.19). The long-range positional correlations of the defects are also lost on increasing the temperature. Microscopy observations show that the pseudoisotropic regions in the lamellar phase (where the optic axis is normal to the substrate) are retained in the lower temperature ordered phase. This observation indicates that both these phases are optically uniaxial [21]. The x-ray data from the defect-ordered phase can be indexed on a 3-D tetragonal lattice with a body centred unit cell ($h + k + l$ is an even integer) (Table 4.1). This lattice is also optically uniaxial. The gradual development of defect correlations, and optical uniaxiality suggest a clear structural relation between the lamellar and tetragonal phases. The repeat period (d) of bilayers in the Ł$_\alpha^D$ phase almost matches the thickness of the primitive unit cell ($c/2$) of the tetragonal phase

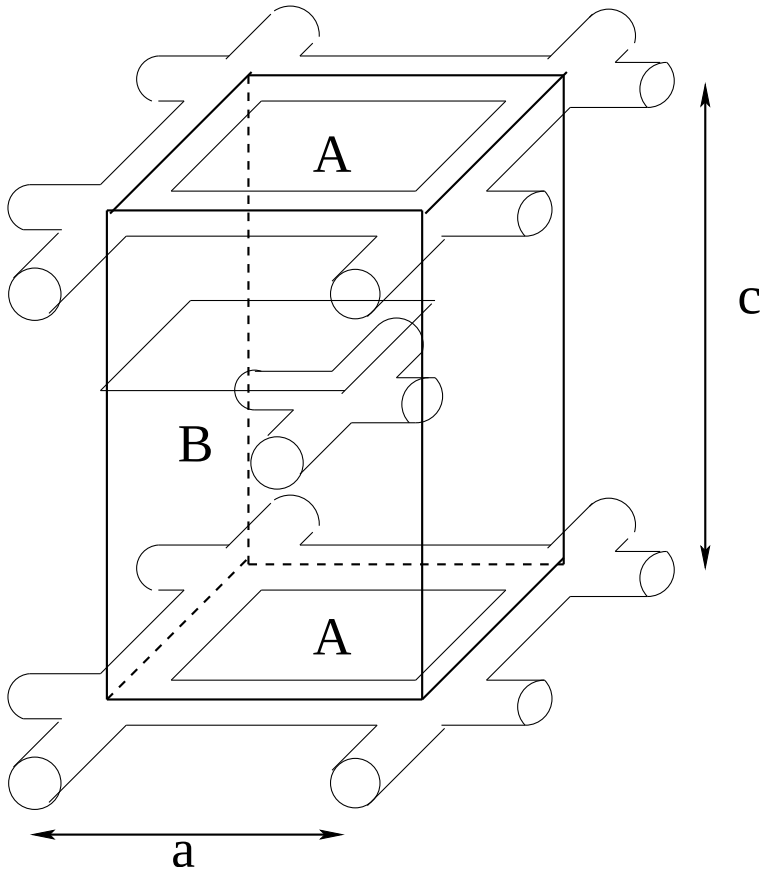

Figure 4.20: Model for the ordered mesh phase indicating the tetragonal unit cell.

(T).

Ordered mesh phase having tetragonal symmetry has been observed in other systems also [22, 23] (Fig. 4.20). The structure is made up of a square lattice of rods. In each unit, four cylindrical micelles meet at a node at right angles to each other to form a 2-D mesh. The meshes are stacked with a two layer repeat with the centres of the squares in one layer placed on top of the nodes in the next. On dilution, the 2-D meshes swell apart to form a lamellar structure where positional correlations across the bilayers are lost. Heating can also have a similar effect. Hence, the basic structural unit of the random mesh phase (L_α^D) and the ordered mesh phase (T) are the same.

To verify the above structure the dimensions of the surfactant aggregates can be calculated from the known volume fraction, as was done in chapter 3. Assuming circular cylinders meeting four by four at each junction (Fig. 4.21), the total volume of the rods in each unit cell can be equated to the surfactant volume fraction in the sample. The length of the cylindrical segment l can be expressed

in terms of the lattice parameter a and the micellar radius r_m as,

$$l = (a - 2r_m). \tag{4.1}$$

In each unit cell of 2-D mesh, there are two rods and one junction. The volume of this unit is given by,

$$v = 2\pi r_m^2(a - 2r_m) + 8r_m^3, \tag{4.2}$$

The volume of surfactant found from the experimental lamellar spacing (d) and the volume fraction of surfactant taken for the sample (ϕ_v) can be equated to the above expression.

$$2\pi r_m^2(a - 2r_m) + 8r_m^3 = a^2 d\phi_v \tag{4.3}$$

ϕ_v was estimated from ϕ_s and the densities of the constituent chemicals. In the above expression $a = d_d$ for L_α^D phase and $d = c/2$ in the T phase. The values of the radius of the cylindrical micelle calculated using this expression are given in table 4.5. The calculated value ($\sim 2.0nm$) is comparable to the molecular length of the surfactant reported in literature [24]. The parameter γ which is the ratio of the in-plane periodicity to the stacking periodicity is defined as d_d/d for random mesh phase and $2a/c$ for T phase. There is a nice trend of γ increasing with ϕ_s in the random mesh phase and the transition to the ordered mesh phase occurs at around $\gamma \sim 1.3$. This observation is consistent with some reports in literature [22, 25]. In our previous chapter such an increase of γ with ϕ_s was shown to give rise to an ordered 3-D intermediate phase, whereas the opposite trend did not result in the ordered phase. It seems to be quite clear that to induce an ordered mesh phase γ has to increase with ϕ_s and reach a critical value. The dependence of appearance of random and ordered mesh phases on the γ values has been explained in chapter 3. It is related to the strength of the modulated interaction potential due to the presence of the structural inhomogeneity in the surface plane.

The length of the alkyl chain of the surfactant, which determines the flexibility of the aggregates, is well known to strongly influence the phases formed by the surfactant. CPB has similar

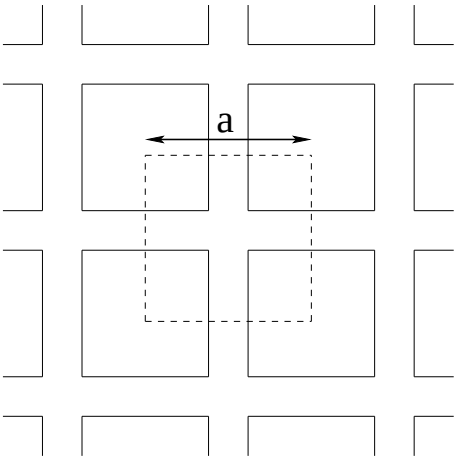

Figure 4.21: Schematic of the square mesh in the random and ordered mesh phases.

Table 4.5: Variation of γ with α and ϕ_s in CPB-SHN-water system. r_m is the micellar radius estimated from the model (Expression (4.3)).$\gamma = d_d/d$ for Ł$^D_\alpha$ phase and $2a/c$ for T phase.

α	ϕ_s	$r_m(nm)$	γ	phase
0.5	40	1.91	1.16	L^D_α
	60	1.94	1.32	L^D_α
	70	1.90	1.30	T
1.0	60	2.04	1.23	L^D_α
	70	1.95	1.25	L^D_α
	80	1.91	1.30	T
1.35	50	1.91	1.10	L^D_α
	60	1.93	1.20	L^D_α
	70	2.02	1.20	L^D_α

chain length as CTAB, but their head group regions differ. In place of the trimethyl ammonium group in CTAB, CPB contains a pyridinium group. The mesh phase in the CTAB-SHN system contains a hexagonal mesh of three coordinated rods whereas the CPB-SHN has a square mesh of four coordinated rods. This suggests the critical role of the head group region of the surfactant in determining the structure of the mesh phase. How this difference produces such a dramatic change is still not clearly understood. It might be related to the local curvature of the surfactant layer which can be tuned by the size and shape of the head group.

4.5.3 Influence of strongly bound counterions

The effect of any added salt to a dilute surfactant system is well studied and is found to induce the formation of long worm-like micelles. Compared to inorganic salts, organic salts are much more efficient to form such aggregates [26]. NMR studies show the organic part of the strongly bound counterions to penetrate into the micellar aggregates projecting only their ionic part into water. In the present studies the salts SS and ST, which contain a benzene ring, could not induce a lamellar phase in the mixtures. Basically they do not change the cylindrical structure of CPB micelles, other than making them longer. SHN containing a naphthalene group is found to transform the cylindrical micelles into mesh-like aggregates. It is not clear if this difference between SHN on the one hand, and SS and ST on the other, is just related to differences in their size, or if other factors, such as their hydrophobicity, are also involved.

4.6 Conclusion

Using microscopy observations and x-ray diffraction studies, the different liquid crystalline phases in the CPB-SHN system have been characterized. A random mesh phase is observed where four rods meet at a junction to give rise to a square array of curvature defects in the plane of the bi-layer. When the meshes are brought closer, by decreasing the water content, they lock in to a 3-D tetragonal lattice. This 3-D ordered phase is found to be destroyed on heating. The radius of the cylinders is calculated from the surfactant volume fraction and is found to be comparable to the molecular length. It is observed that to induce the ordered mesh phase the ratio of the mesh size

to the bilayer separation needs to follow a certain trend. The ternary phase diagram is found to be symmetric about the equimolar composition of CPB and SHN. Unlike the CPB-SHN system, the CPC-SHN system shows only the presence of regular lamellar phase. It is also observed that not all organic salt can indue the mesh phases in these systems. Further experiments are necessary to understand the structural features of the strongly bound counterion that are important in determining the phases in such mixed systems.

Bibliography

[1] U. Henriksson, E. S. Blackmore, G. J. T. Tiddy and O. Soderman *J. Phys. Chem*, **96**, 3894 (1992).

[2] C. Hall and G. J. T. Tiddy In *Surfactant in Solution*, Ed. K. L. Mittal, Plenum Press: New York, vol **1**, 9 (1989).

[3] E. W. Kaler, K. L. Herrington, A. K. Murthy and J. A. N. Zasadzinski *J. Phys. Chem.*, **96**, 6698 (1992).

[4] B. K. Mishra, S. D. Samant, P. Pradhan, S. B. Mishra and C. Manohar *Langmuir*, **9**, 894 (1993).

[5] G. Porte, J. Appel and Y. Poggl *J. Phys. Chem*, **84**, 3105 (1980).

[6] G. Porte and J. Appel *J. Phys. Chem*, **85**, 2511 (1981).

[7] R. Gomati, J. Appell, P. Bassereau, J. Marignan and G. Porte *J. Phys. Chem*, **91**, 6203 (1987).

[8] W. J. Benton and C. A. Miller *J. Phys. Chem*, **87**, 4981 (1983).

[9] A. Auvraay, C. Petipas, T. Perche, R. Anthore, M. J. Marti, I. Rico and A. Lattes *J. Phys. Chem*, **94**, 8604 (1990).

[10] V. Luzzati *Biological Membrane*, Ed. D. Chapman, Academic Press: London and Yew York, *p* 71 (1968).

[11] J. Burgoyne, M. C. Holmes and G. J. T. Tiddy *J. Phys. Chem*, **99**, 6054 (1995).

[12] S. T. Hyde *J. Phys. Chem*, **93**, 1458 (1989).

[13] M. C. Holemes, A. M. Smith and M. S. Leaver *J. Phys. II France*, **3**, 1357 (1993).

[14] M. C. Holemes *Curr. Opin. Clooid Interface Sci*, **3**, 485 (1998).

[15] M. E. Cates and S. J. Candau *J. Phys: Condens. Matter*, **2**, 6869 (1990).

[16] R. Bandyopadhyay and A. K. Sood *Langmuir*, **19**, 3121 (2003).

[17] P. A. Hassan, S. R. Raghavan and E. W. Kaler *Langmuir*, **18**, 2543 (2002).

[18] V. Hartmann and R. Cressely *J. Phys II France*, **7**, 1087 (1997).

[19] M. R. Rizzatti and J. D. Gault *Colloid Interface Sci*, **110**, 258 (1987).

[20] H. I. Petrache, I. Kimchi, D. Harries and V. A. Parsegian *J. Am. Chem. Soc*, **127**, 11546 (2005).

[21] S. K. Ghosh, R. Ganapathy, R. Krishnaswamy, J. Bellare, V. A. Raghunathan and A. K. Sood *Langmuir*, **23**, 3606 (2007).

[22] P. Kekicheff and G. J. T. Tiddy *J. Phys. Chem*, **93**, 2520 (1989).

[23] V. Luzzati, A. Tardieu and T. Gulik-Krzwicki *Nature*, **217**, 1028 (1968).

[24] F. Reiss-Husson and V. Luzzati *J. Phys. Chem*, **68**, 3504 (1964).

[25] S. Puntambekar, M. C. Holmes and M. S. Lever *Liq. Cryst*, **27**, 3504 (2002).

[26] G. Garg, P. A. Hassan, V. K. Aswal and S. K. Kulshrestha *J. Phys. Chem. B*, **109**, 1340 (2005).